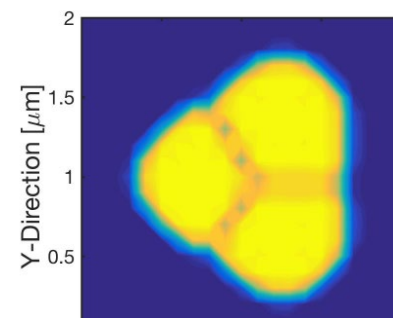
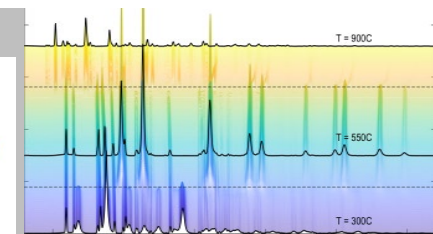
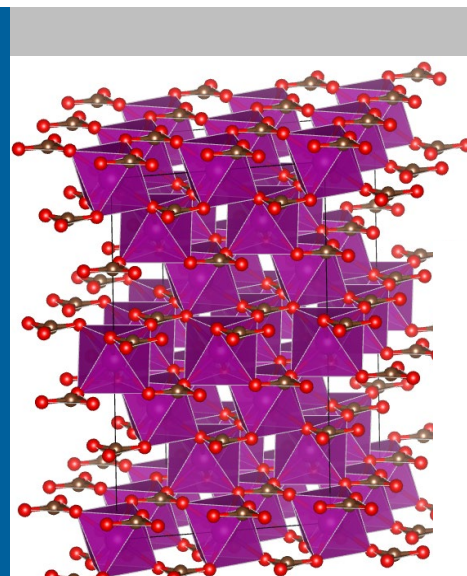


THIS PRESENTATION DOES NOT CONTAIN ANY PROPRIETARY,
CONFIDENTIAL, OR OTHERWISE RESTRICTED INFORMATION



IMPROVING BATTERY PERFORMANCE THROUGH STRUCTURE- MORPHOLOGY OPTIMIZATION



VENKAT SRINIVASAN

Argonne National Laboratory, Lemont, IL

CONTRIBUTORS:

HAKIM H. IDDIR

PALLAB BARAI

JUAN C. GARCIA

TIMOTHY T. FISTER

Project ID: **BAT402**

Date: June 10th – 13th, 2019

Location: Arlington, VA

OVERVIEW

Timeline

- Start date: October 2018
- End date: September 2021
- Percent complete: 16%

Barriers

- Barriers addressed
 - Size, shape, porosity, tap density and reactivity of primary and secondary particles during coprecipitation of cathode precursors.
 - Densification issues during sintering of LLZO pellets.

Budget

- **\$450k/year**
 - 0.5 FTE Staff Scientist
 - 1.5 FTE Postdoc

Partners

- Greg Krumdick and Joseph Libera (MERF, ANL), Project ID: BAT315
- Jason Croy and Arturo Gutierrez (ANL)
- Kenneth Higa (LBNL)
- Feng Wang (BNL), Project ID: BAT183
- Joanne Stubbs and Peter Eng. (APS)

RELEVANCE

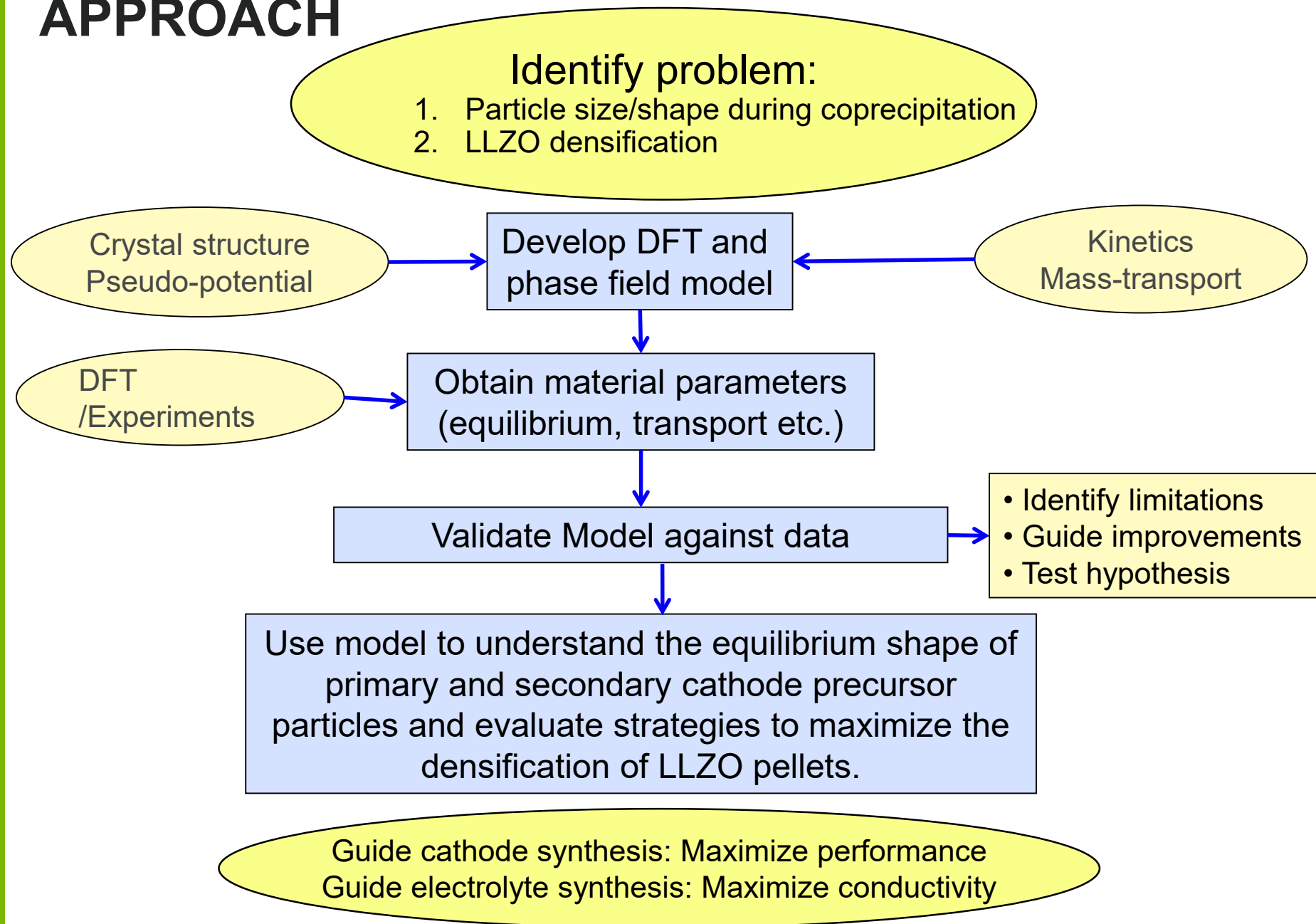
Objectives:

- Investigate the impact of solution pH, ammonia content, and transition metal concentration on the size, shape, porosity, tap density and facet dependent reactivity of cathode precursors during the coprecipitation process.
 - Determine the equilibrium Wulff shape and corresponding surface energies of cathode precursors and final materials.
 - Elucidate the impact of thermodynamic and kinetic factors in determining the size and shape of primary and secondary particles.
- Elucidate the densification and grain growth mechanism observed during the sintering of LLZO pellets.
 - Develop phase-field based mesoscale models capable of capturing the sintering process between multiple LLZO particles.
 - Experimentally measure the densification and growth of LLZO particles during the sintering process.

MILESTONES

Serial no.	Milestone description	Completion date	Status
1	Model impact of sintering temperature on the densification observed in LLZO solid-state electrolytes	31 st December, 2018	Completed
2	For Mn-rich carbonate precursors, start with MnCO_3 low energy facets, and determine the surface energy of various facets	15 th February, 2019	Completed
3	Experimentally estimate the effect of sintering on the densification and size of LLZO particles	31 st March, 2019	Completed
4	Investigate the effect of O and H coverage (pH, and other synthesis conditions) and surface terminations on the Wulff shape	15 th April, 2019	Completed
5	Estimate growth of Mn-rich carbonate primary and secondary particles with facet dependent surface energy and precipitation kinetics	30 th June, 2019	In progress
6	Quantify facet-specific growth of precursor particles by using X-ray scattering techniques	30 th September	No started

APPROACH



DETAILS ABOUT THE COMPUTATIONAL MODEL

Phase field based governing equations for facet dependent growth of primary particles:

- Phase field equation:
$$\tau \frac{\partial \phi}{\partial t} = \varepsilon^2 \nabla^2 \phi - \frac{\partial f}{\partial \phi} \quad \begin{array}{l} \phi = -1 \rightarrow \text{Solid} \\ \phi = +1 \rightarrow \text{Liquid} \end{array}$$
- Orientation dependence incorporated into the model as: $\varepsilon = \varepsilon(\vec{n}) \quad \vec{n} : \text{Normal direction}$
- Anisotropic: $\varepsilon = \max(\hat{n} \cdot \vec{\eta}_k) \quad \eta_k : \text{Directions of corners of Wulff shape}$

Phase field equations for predicting the high temperature sintering process:

Free energy functional:
$$F = \int_V \left[\underbrace{f(\rho, \eta_\alpha)}_{\text{Bulk chemical free energy}} + \underbrace{\frac{1}{2} \beta_\rho |\nabla \rho|^2}_{\text{Gradient energy at solid-pore domain}} + \sum_\alpha \underbrace{\frac{1}{2} \beta_\eta |\nabla \eta_\alpha|^2}_{\text{Gradient energy at the boundary of individual grains}} \right]$$

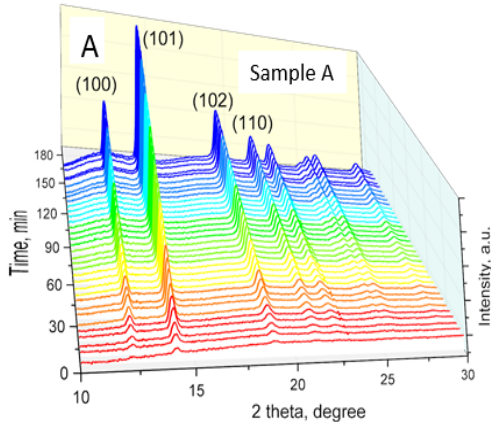
Evolution of solid-pore domain: $\frac{\partial \rho}{\partial t} = \nabla \cdot \left(D \nabla \frac{\delta F}{\delta \rho} - \rho \vec{v}_{adv} \right)$ Evolution of grain/grain-boundary microstructure: $\frac{\partial \eta_\alpha}{\partial t} = -L \frac{\delta F}{\delta \eta_\alpha} - \nabla \cdot (\eta_\alpha \vec{v}_{adv}(\alpha))$

Atomistic analysis using the Density Functional Theory (DFT):

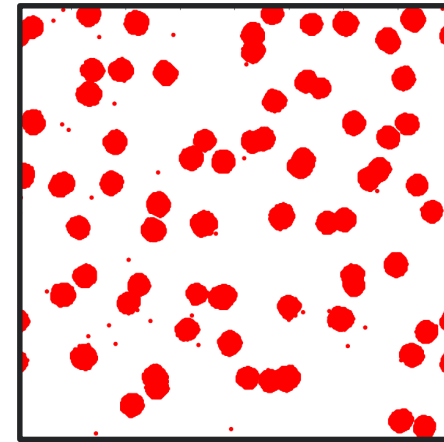
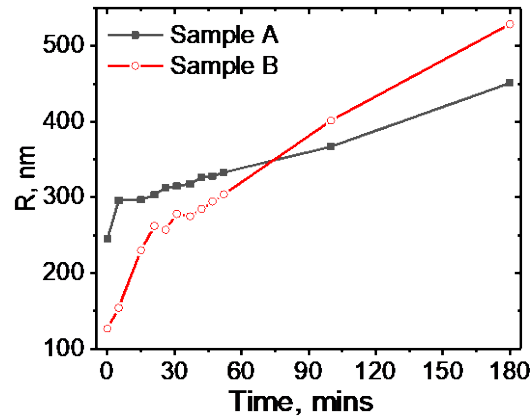
- All calculations conducted by spin polarized DFT as implemented in Vienna Ab Initio Simulation Package (VASP)
- Exchange correlation potentials are treated by generalized gradient approximation (GGA)
- Interaction between valence electron and ion core described by projected augmented wave (PAW) method.

TASK:1. SYNTHESIS OF CATHODE PARTICLES

Where were we in October 2018



Feng et al., JES (2018) 165, A3077



Barai et al., JPCB (2019) 123, 15, 3291

Measure particle size evolution:

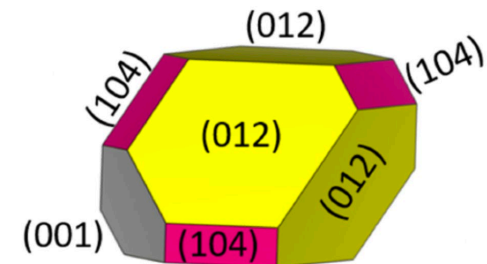
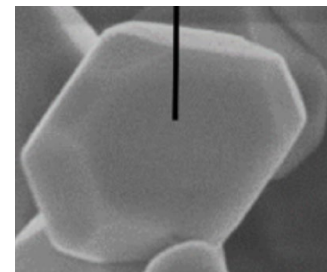
- *In situ* visualization of crystal phase formation
- Measure primary and secondary particle size

Model coprecipitation:

- Growth of primary particles
- Formation of secondary particles

But:

1. Primary particles are often not spherical.
2. Growth is not symmetric.
3. Final shape of particle used in battery is after sintering, not just co-precipitation.
4. There is chemistry accompanying the morphological changes.



Garcia et al., JPCC (2017) 121, 8290

Estimation of Wulff shape of primary particles

UNDERSTANDING HOW PRECURSORS IMPACT PARTICLE SHAPE

Coprecipitation process affects the formation of primary and secondary particles

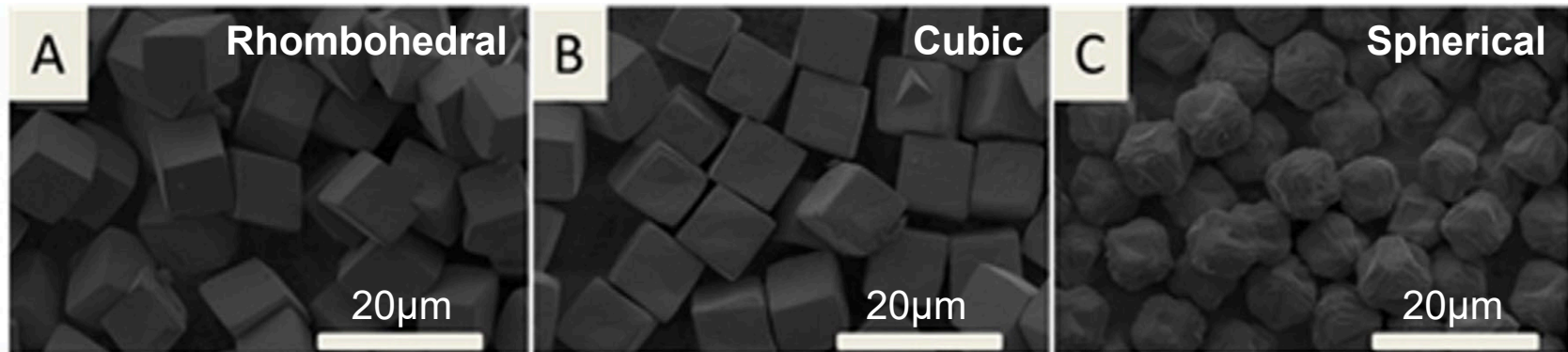
Hydroxide precursors:

- ❑ Better control over secondary particle size and tap density for NMC 111 and Ni-rich cathodes
- ❑ But, Mn rich hydroxide precursors oxidize to Mn-oxy-hydroxides, which tends to phase separate

Carbonate precursors:

- ❑ Carbonates are cheap
- ❑ But, less control over the particle size and tap-density

- Effect of Mn^{2+} concentration in solution on particle shape



Robinson and Koenig, *Powder Tech.* 2015 284 225 - 230

Increasing MnSO_4 in the solution

We are using NMC precursors as a test bed to understand why primary particle shape changes

EQUILIBRIUM EQUATIONS FOR COPRECIPITATION PROCESS

List of equilibrium equations:

Wang et al., J. Mater. Chem., 2011, 21, 9290

Table 1 Equilibrium reactions and constants used in calculation of the residual transition metals in the solution

Equilibrium reactions	Equilibrium constant K
$\text{H}_2\text{CO}_3 \leftrightarrow \text{H}^+ + \text{HCO}_3^-$	4.3×10^{-7}
$\text{HCO}_3^- \leftrightarrow \text{H}^+ + \text{CO}_3^{2-}$	5.62×10^{-11}
$\text{MnCO}_3 \leftrightarrow \text{Mn}^{2+} + \text{CO}_3^{2-}$	2.34×10^{-11}
$\text{NiCO}_3 \leftrightarrow \text{Ni}^{2+} + \text{CO}_3^{2-}$	1.42×10^{-7}
$\text{Mn}^{2+} + n\text{NH}_3 \leftrightarrow [\text{Mn}(\text{NH}_3)_n]^{2+}$	See ref.16
$\text{Ni}^{2+} + n\text{NH}_3 \leftrightarrow [\text{Ni}(\text{NH}_3)_n]^{2+}$	See ref.16
$\text{Mn}(\text{OH})_2 \leftrightarrow \text{Mn}^{2+} + 2\text{OH}^-$	1.9×10^{-13}
$\text{Ni}(\text{OH})_2 \leftrightarrow \text{Ni}^{2+} + 2\text{OH}^-$	5.48×10^{-16}
$\text{NH}_3 \cdot \text{H}_2\text{O} \leftrightarrow \text{NH}_4^+ + \text{OH}^-$	5.7×10^{-10}
$\text{H}_2\text{O} \leftrightarrow \text{OH}^- + \text{H}^+$	10^{-14}

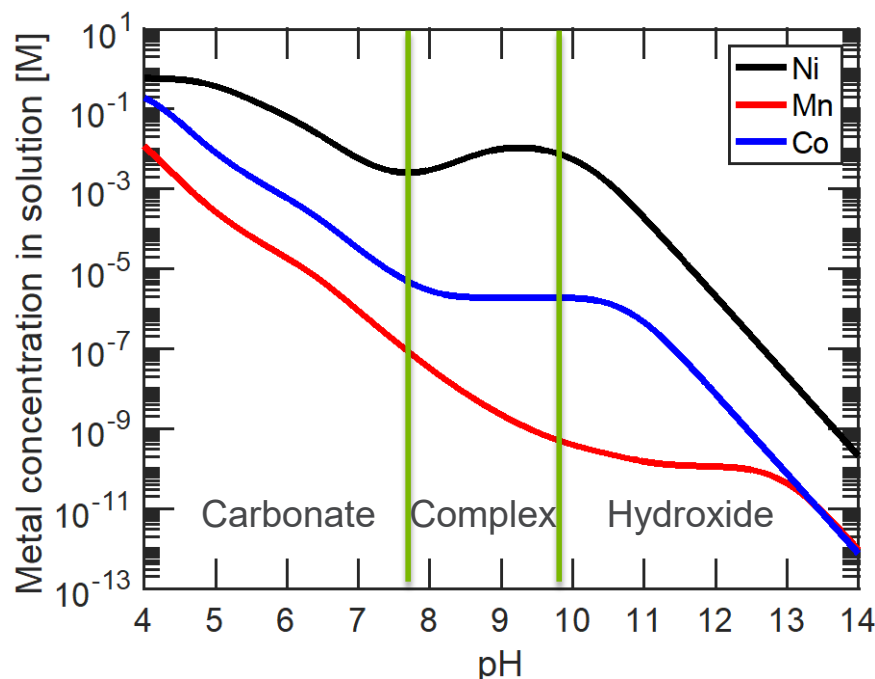
Van Bommel and Dahn, Chem. Mater. 2009, 21, 1500

Table 2. Equilibria and Mass Balances Solved to Determine the Concentration of Species Present in the Reactor at Various pH Values

equilibrium reaction	K	log K		
		Ni	Mn	Co
$\text{M}^{2+} + \text{NH}_3 \rightleftharpoons [\text{M}(\text{NH}_3)]^{2+}$	K_1	2.81	1.00	2.10
$\text{M}^{2+} + 2\text{NH}_3 \rightleftharpoons [\text{M}(\text{NH}_3)_2]^{2+}$	K_2	5.08	1.54	3.67
$\text{M}^{2+} + 3\text{NH}_3 \rightleftharpoons [\text{M}(\text{NH}_3)_3]^{2+}$	K_3	6.85	1.70	4.78
$\text{M}^{2+} + 4\text{NH}_3 \rightleftharpoons [\text{M}(\text{NH}_3)_4]^{2+}$	K_4	8.12	1.3	5.53
$\text{M}^{2+} + 5\text{NH}_3 \rightleftharpoons [\text{M}(\text{NH}_3)_5]^{2+}$	K_5	8.93		5.75
$\text{M}^{2+} + 6\text{NH}_3 \rightleftharpoons [\text{M}(\text{NH}_3)_6]^{2+}$	K_6	9.08		5.14
$\text{NH}_3 + \text{H}_2\text{O} \rightleftharpoons \text{NH}_4^+ + \text{OH}^-$	K_b	-4.80	-4.80	-4.80
$\text{M}(\text{OH})_2 \rightleftharpoons \text{M}^{2+} + 2\text{OH}^-$	K_{sp}	-15.22	-12.70	-14.89
$\text{H}_2\text{O} \rightleftharpoons \text{H}^+ + \text{OH}^-$	K_w	-14	-14	-14

Coprecipitation of cathode precursors

Mass balance equation for the reacting ions within the solution have been solved.

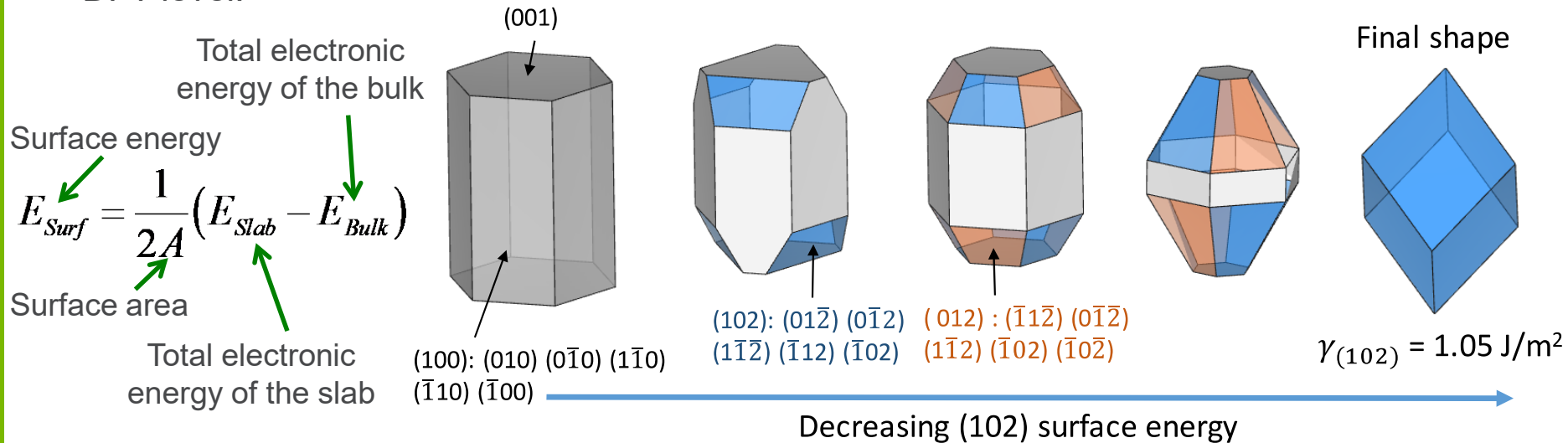


Desired pH for coprecipitation:

- Carbonate precursors: $7.5 < \text{pH} < 8.5$
- Hydroxide precursors: $\text{pH} > 10.0$

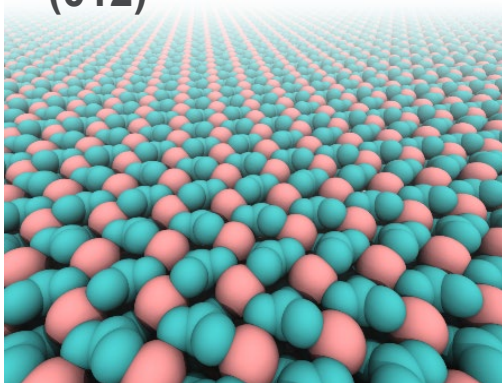
WULFF SHAPES OF PRECURSOR PRIMARY PARTICLES: DFT CALCULATIONS

- Cleavage energy for most relevant facets in carbonate precursors were calculated at the DFT level:

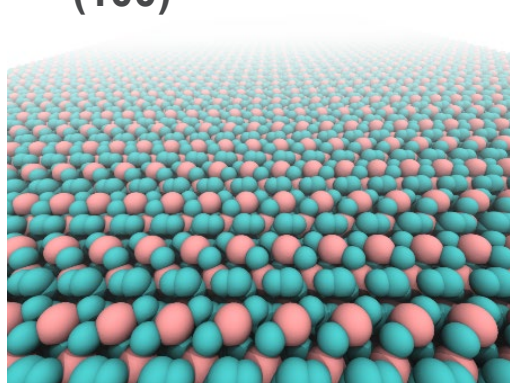


Precursor Surface models:

(012)

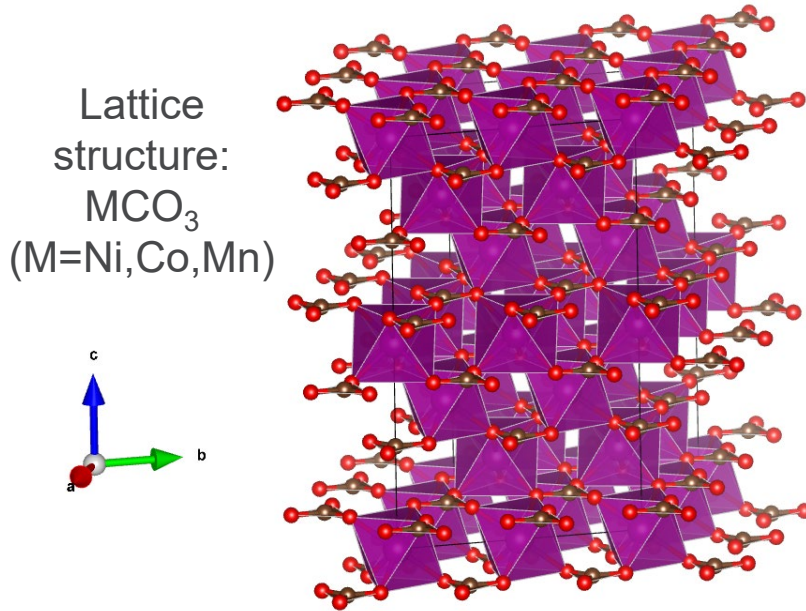


(100)

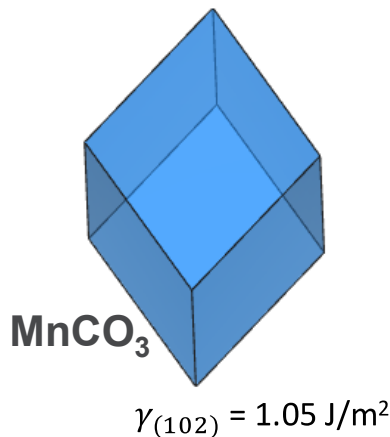


The metal carbonates precursors shape is dominated by the low energy facet (102) at high pH.

WULFF SHAPES OF CARBONATE PRECURSOR PRIMARY PARTICLES: DFT CALCULATIONS



Wulff shape of particle with lowest energy surface (102):



Robinson and Koenig, *Powder Tech.* 2015 284 225 - 230

Surface energy of different transition metal carbonates

		Surface area (\AA^2)	surface energy (J/m^2)
MnCO_3	S100	74.66	2.00
	S001	39.46	2.90
	S012	108.64	2.29
	S102	36.21	1.05
NiCO_3	S100	68.01	2.74
	S001	36.83	2.39
	S012	108.64	2.29
	S102	33.42	1.79
CoCO_3	S100	69.63	2.46
	S001	37.90	2.04
	S012	108.64	2.33
	S102	34.31	1.53

Equilibrium shapes of carbonate precursors estimated from the DFT calculations correlate well with experiment.

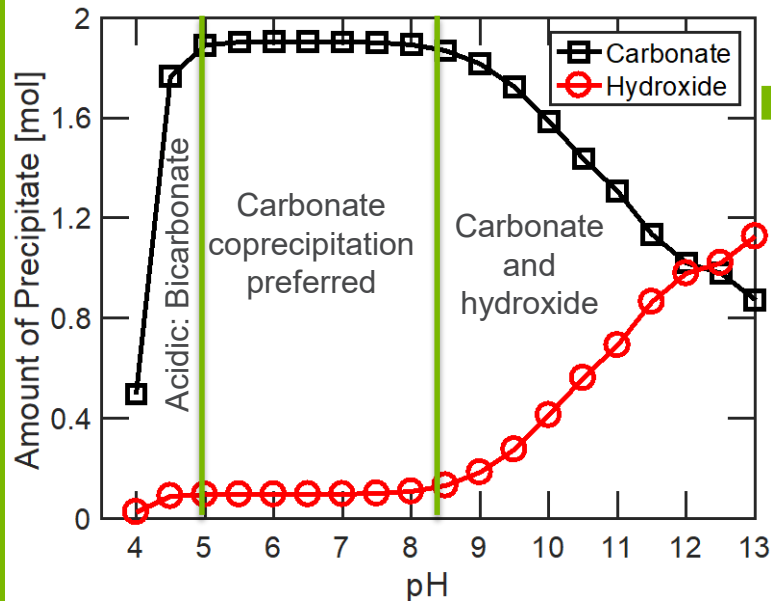
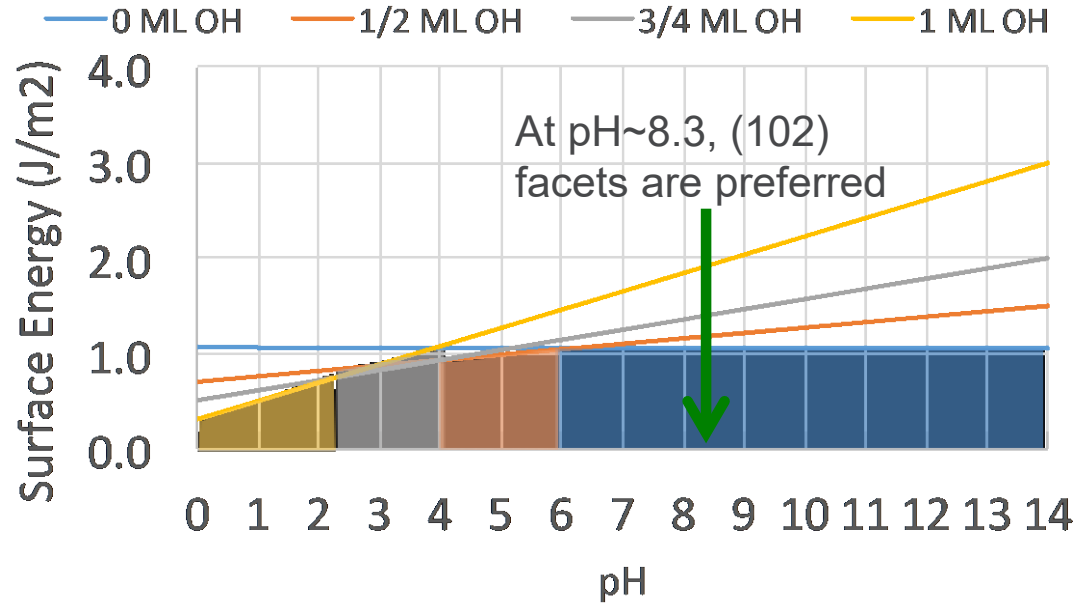
DFT to continuum:

- ☐ Equilibrium Wulff shape of primary particles
- ☐ Surface energy densities

EFFECT OF SOLUTION PH ON THE SHAPE OF PRIMARY PARTICLE

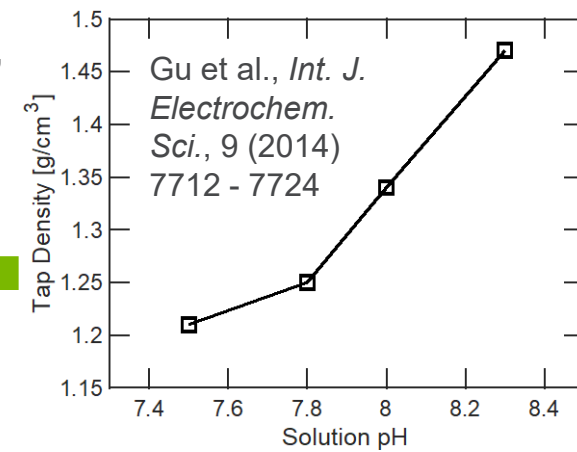
The (102) surface is polar, hence its energy will depend on the solution pH.

For solution pH > 6.0, no significant change in the surface energy of (102) facets.



To minimize hydroxides, pH < 8.5 is preferred

To maximize tap density, pH > 8.0 is preferred



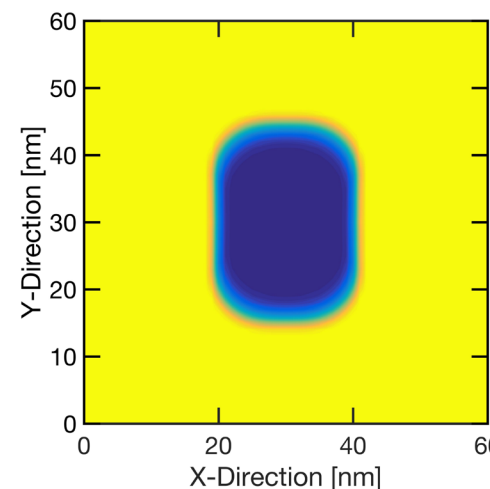
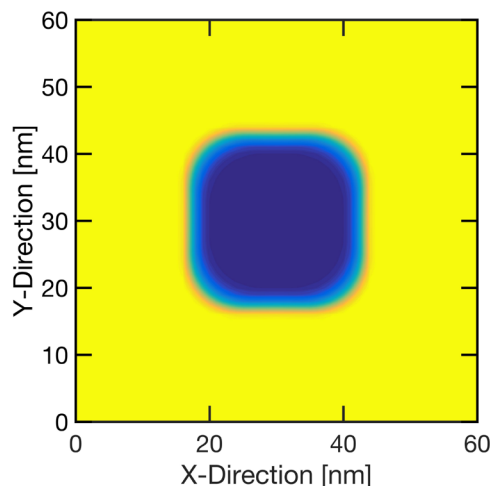
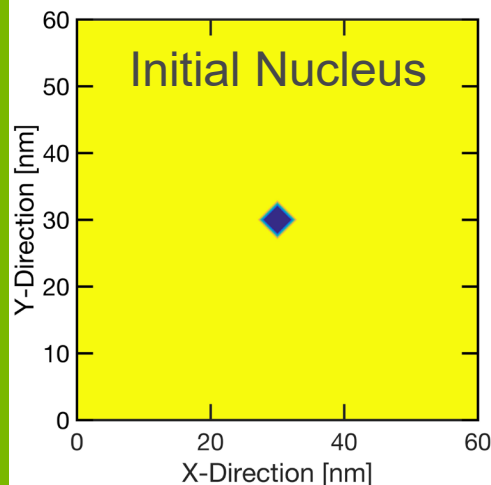
Model providing some insights already

GROWTH OF PRECIPITATES WITH DIFFERENT WULFF SHAPE

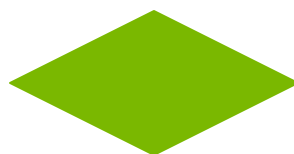
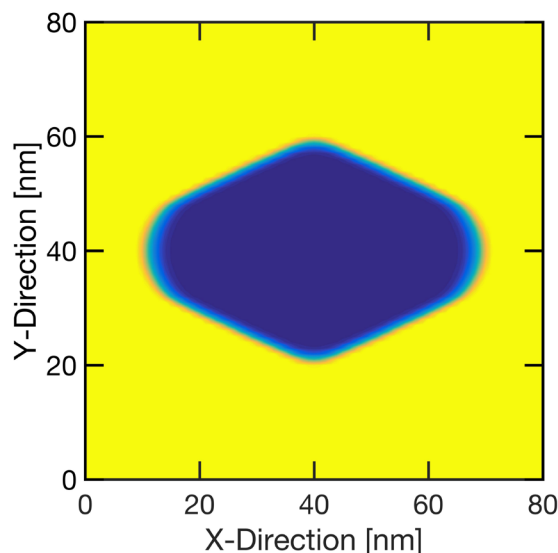
From the nucleus state, growth of primary particles depend on:

- **Kinetics:** Reaction rate and diffusion of particles
- **Thermodynamics:** Wulff shape of the particles, surface energy

Focus on capturing facets during growth of primary particles



(Green squares represent the respective Wulff shapes)

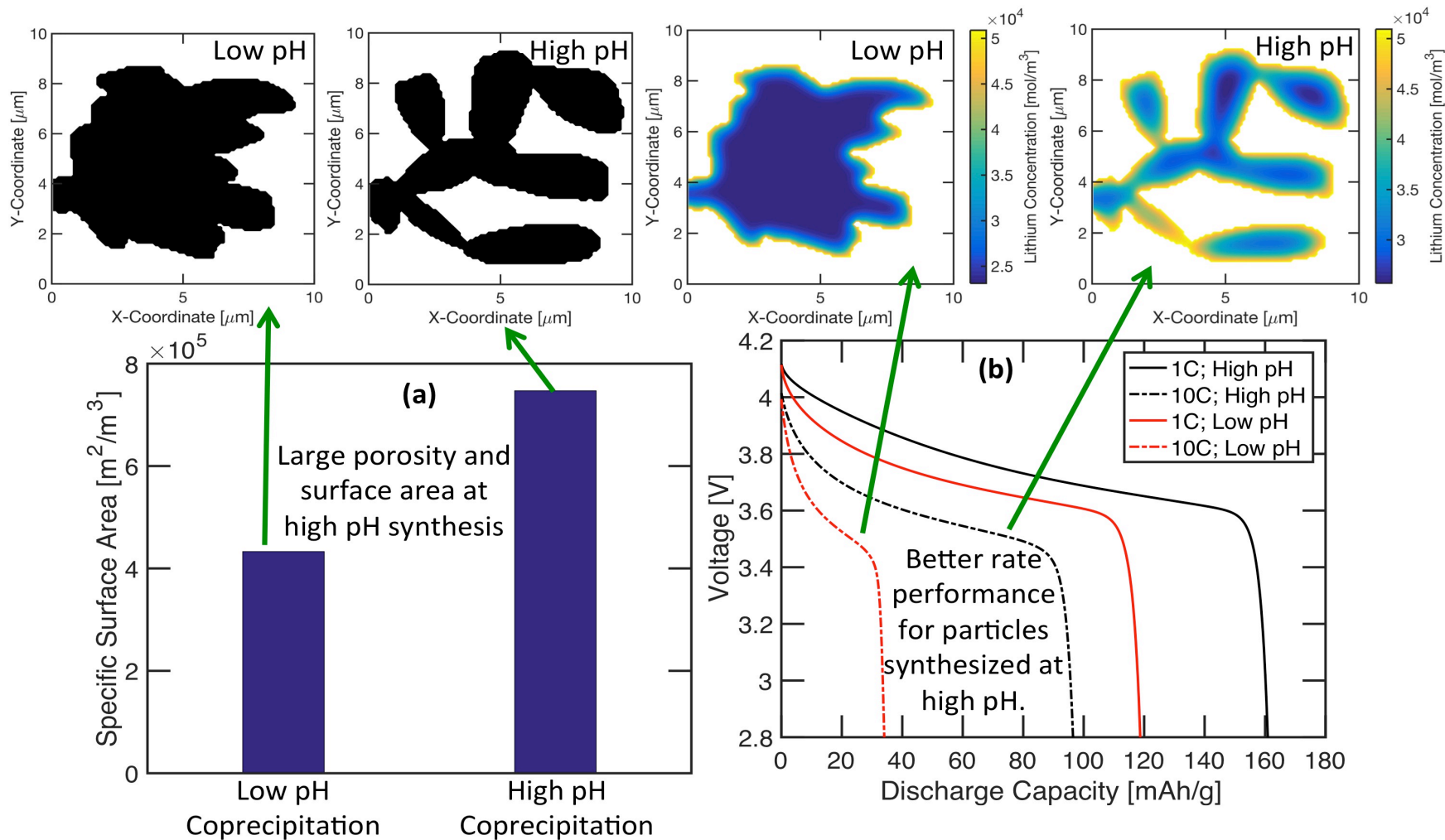


Wulff shape for carbonate precursors as predicted by DFT.

Facet dependent growth of primary particles successfully captured by the developed computational model.

LINKING MORPHOLOGY TO PERFORMANCE

Microstructure model (more details than averaging-type “Newman” model)



Larger internal porosity of the secondary particles provide more surface area for electrochemical reaction, which leads to higher initial capacity as well as side reaction.

TASK: 1. FUTURE WORK POSSIBILITIES

Develop a better understanding of how solution metal concentration affects the:

- Shape of the primary particles.
- Size of the primary and secondary particles

Analysis of secondary particle growth dynamics:

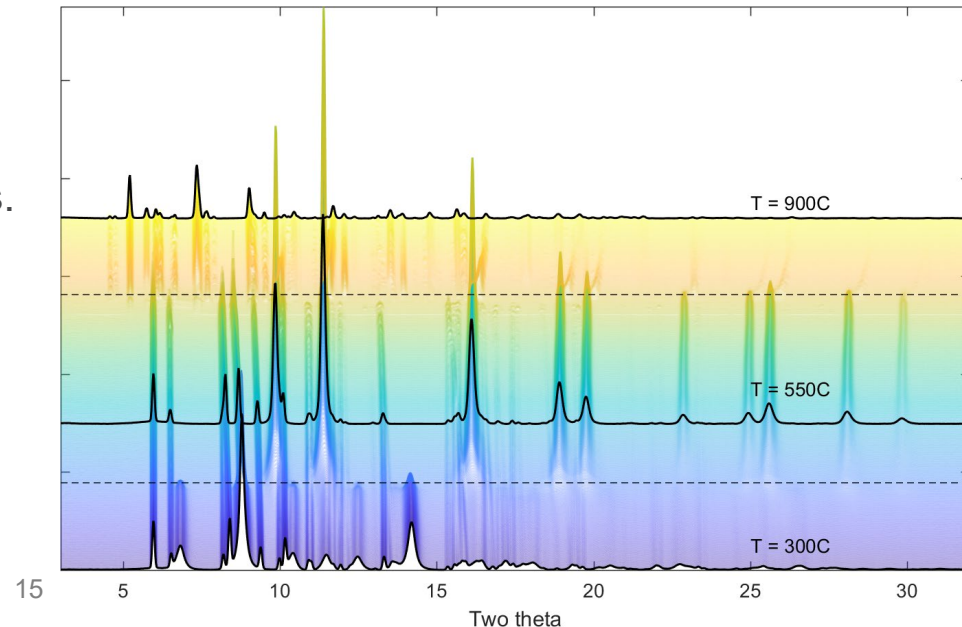
- Carbonate precursors usually lead to large secondary particles (~ 20 microns diameter). Try to understand the reason behind the bigger size of the secondary particles through experiments and computational analysis.

Model development to understand the calcination of carbonate precursors:

- Develop models to understand the oxidation and lithiation of transition metals.
- Develop methodologies for predicting the size changes during sintering.

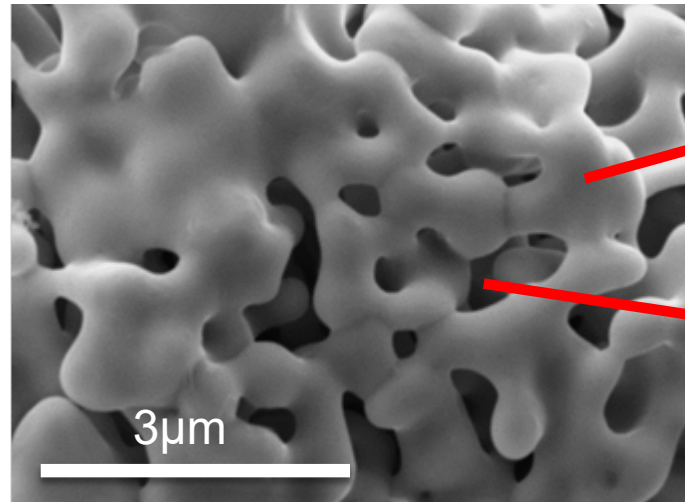
Calcination (conducted at APS).

1. Formation of rock salt (nano phase)
2. Growth of the oxide



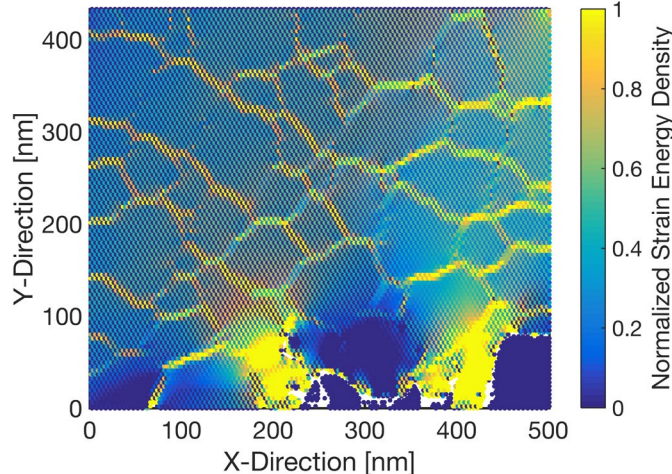
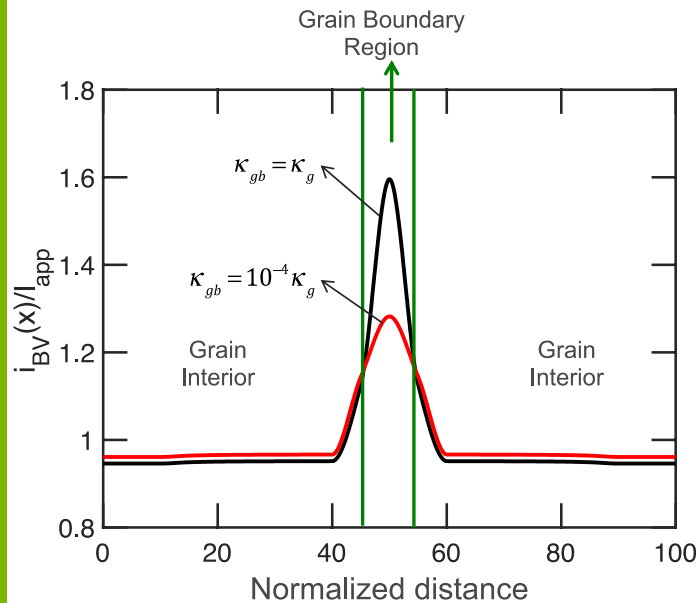
TASK: 2. LLZO SOLID STATE ELECTROLYTE: DENSIFICATION AND GRAIN STRUCTURE

SEM image of LLZO particles after annealing for 12 hours (Source: Joe Libera (MERF, ANL), Project ID: BAT315)



Sintered LLZO particles

Void space

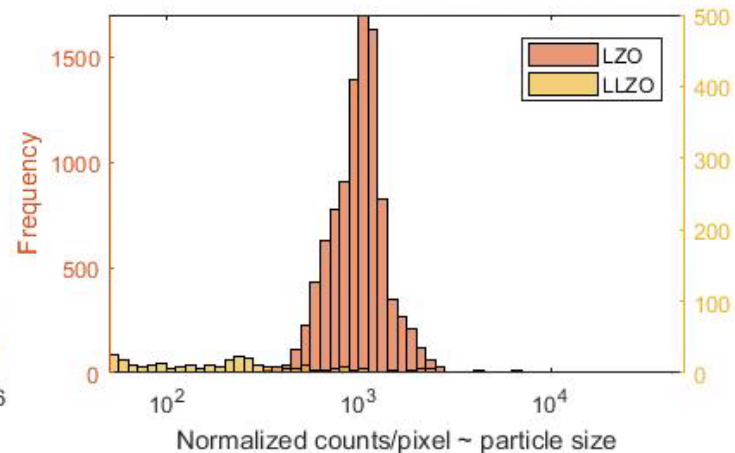
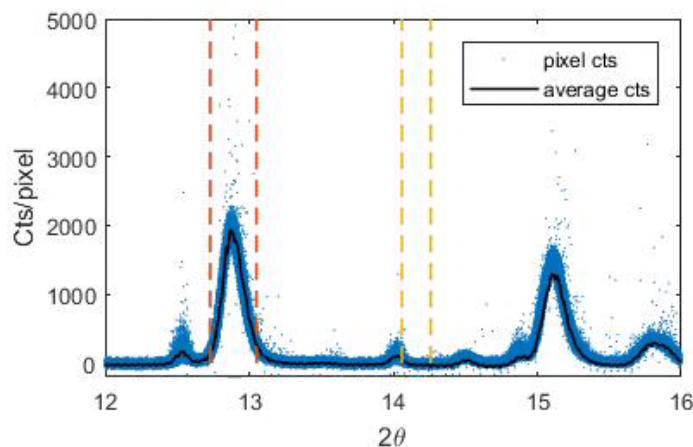
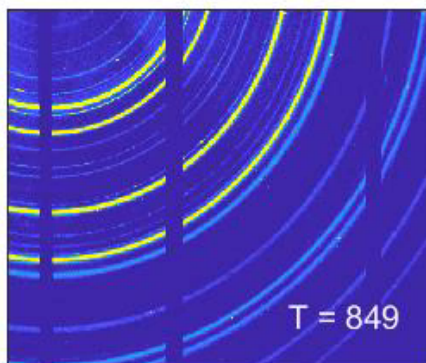


Current focusing and propensity of fracture initiation at the grain-boundary region (Source: Srinivasan et al., Project ID: BAT309)

Investigate the synthesis of LLZO in order to maximize conductivity and minimize current focusing at the grain-boundary regions.

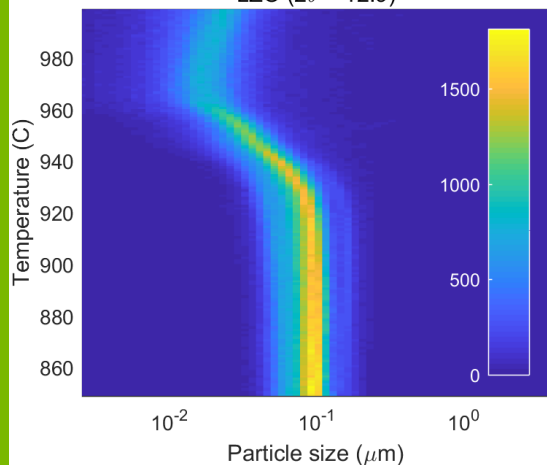
EXPERIMENTAL RESULTS: LLZO DENSIFICATION

Calcination of green powder (obtained from MERF, ANL) conducted at APS to understand the formation of cubic LLZO phase and grain ripening. (Temperature ramp rate: $10^{\circ}\text{C}/\text{min}$)



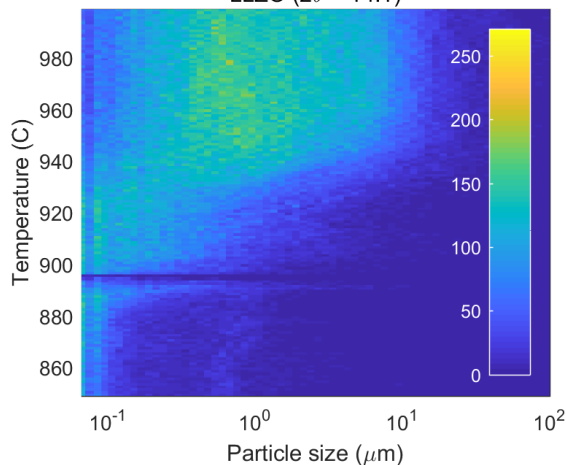
LZO precursors: $D_{\text{avg}} \sim 100\text{nm}$

LZO ($2\theta = 12.9$)



LLZO: Major ripening starts at 940°C

LLZO ($2\theta = 14.1$)



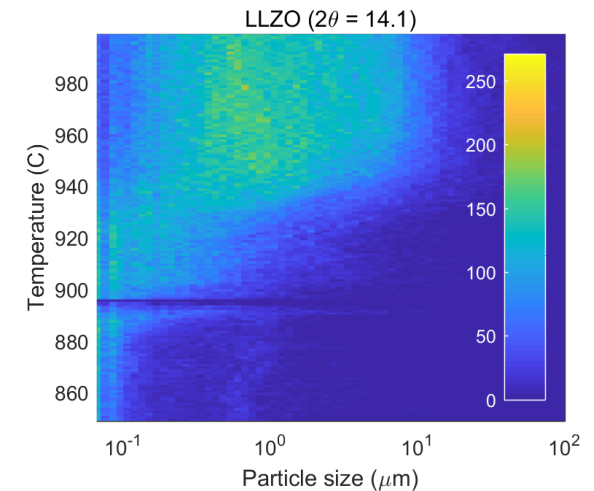
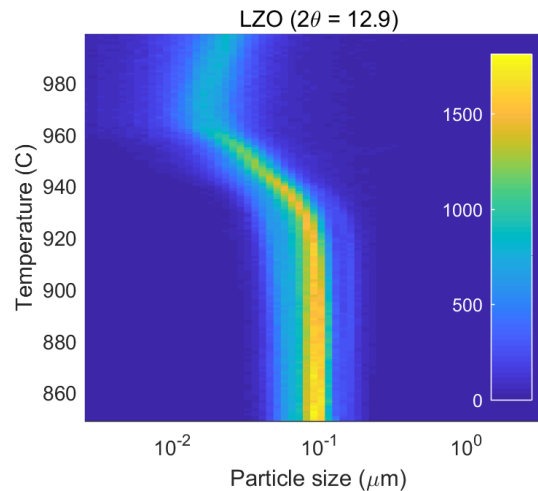
With increasing temperature, LZO reacts with Li_2CO_3 and forms LLZO, which experiences further grain growth.

Input for computational model:

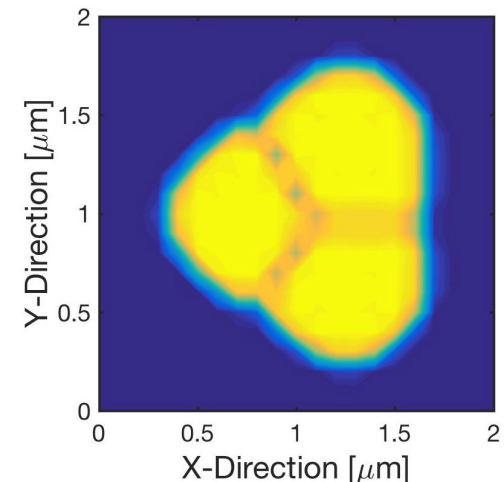
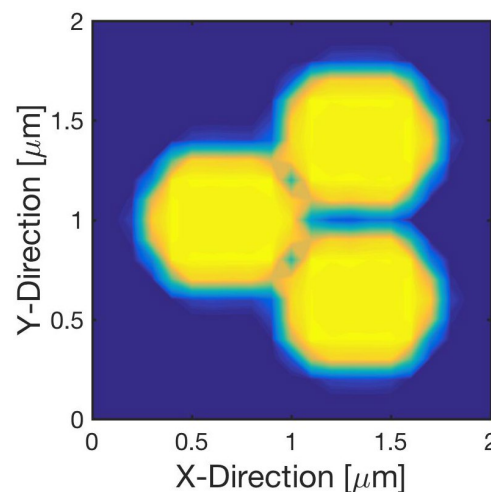
- Initial size of LLZO is assumed to be 100nm.

MODELING OF SINTERING PROCESS TO PREDICT DENSIFICATION AND PARTICLE SIZE EVOLUTION

In situ sintering to track particle size (Conducted at the APS)



Modeling particle morphology during sintering



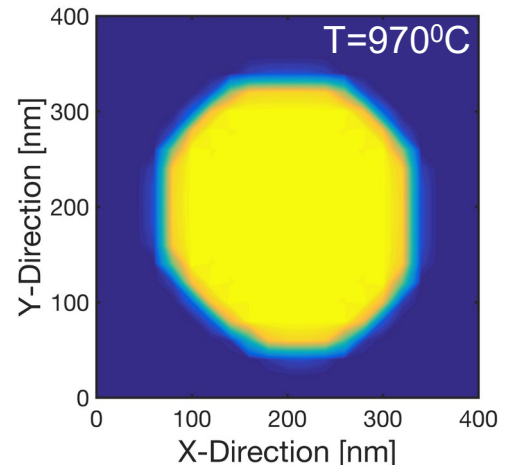
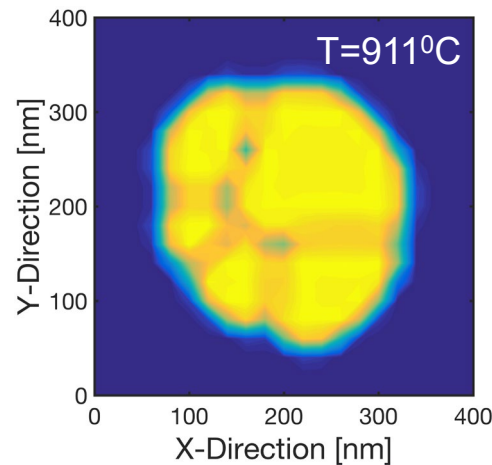
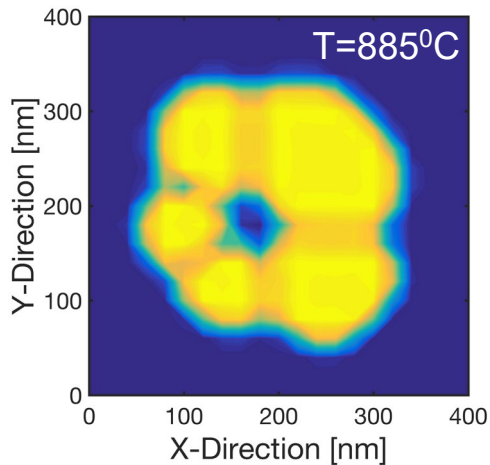
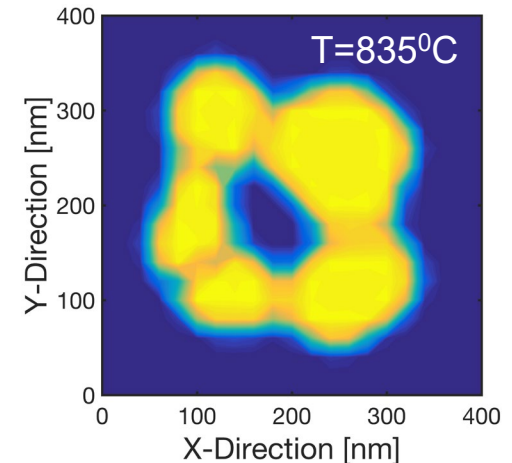
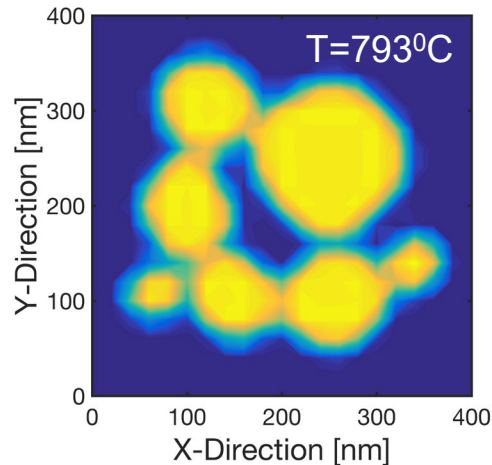
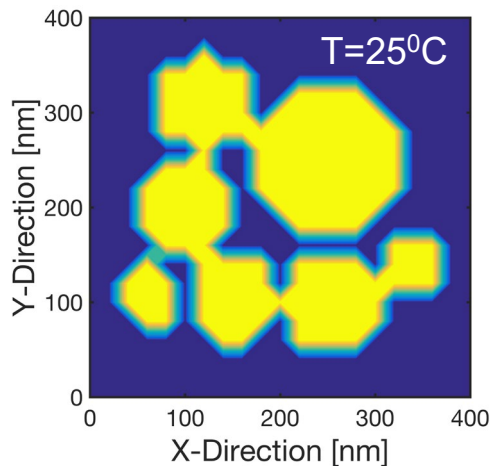
The developed phase field model successfully captures densification and grain growth processes.

LLZO GRAIN GROWTH WITH EXPERIMENTALLY OBSERVED PARTICLE SIZE

Temperature ramp
rate: $10^{\circ}\text{C}/\text{min}$

Average initial particle
size: $D_{\text{avg}} \sim 100\text{nm}$

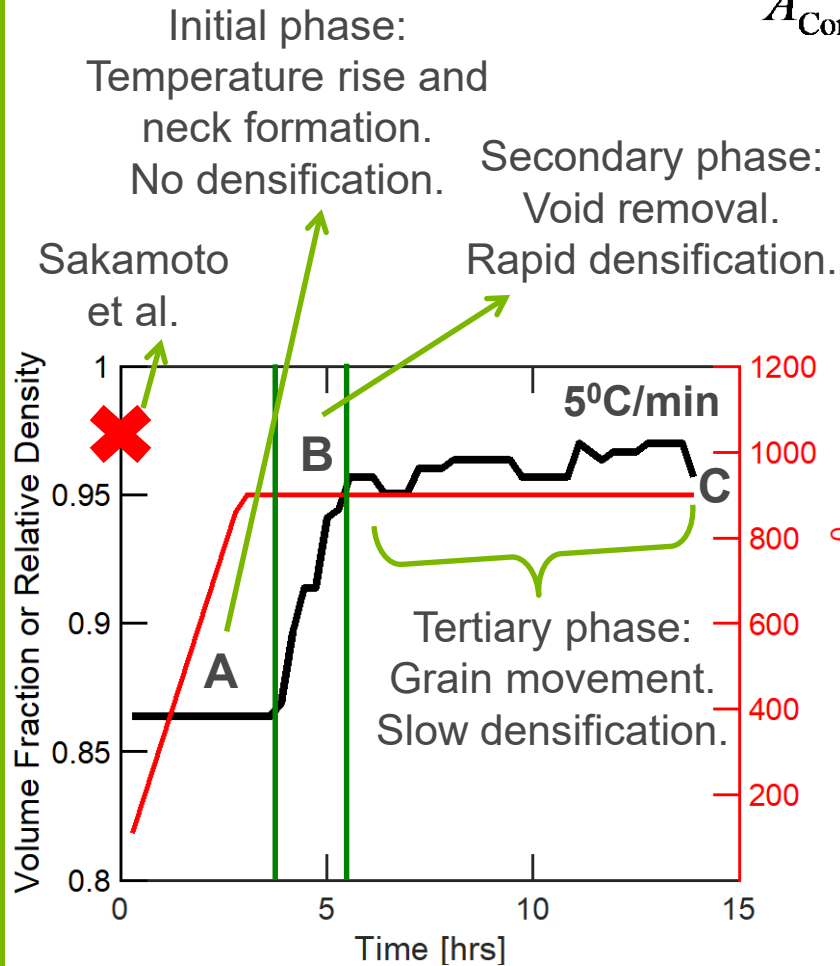
Final particle size:
280nm @ 970°C



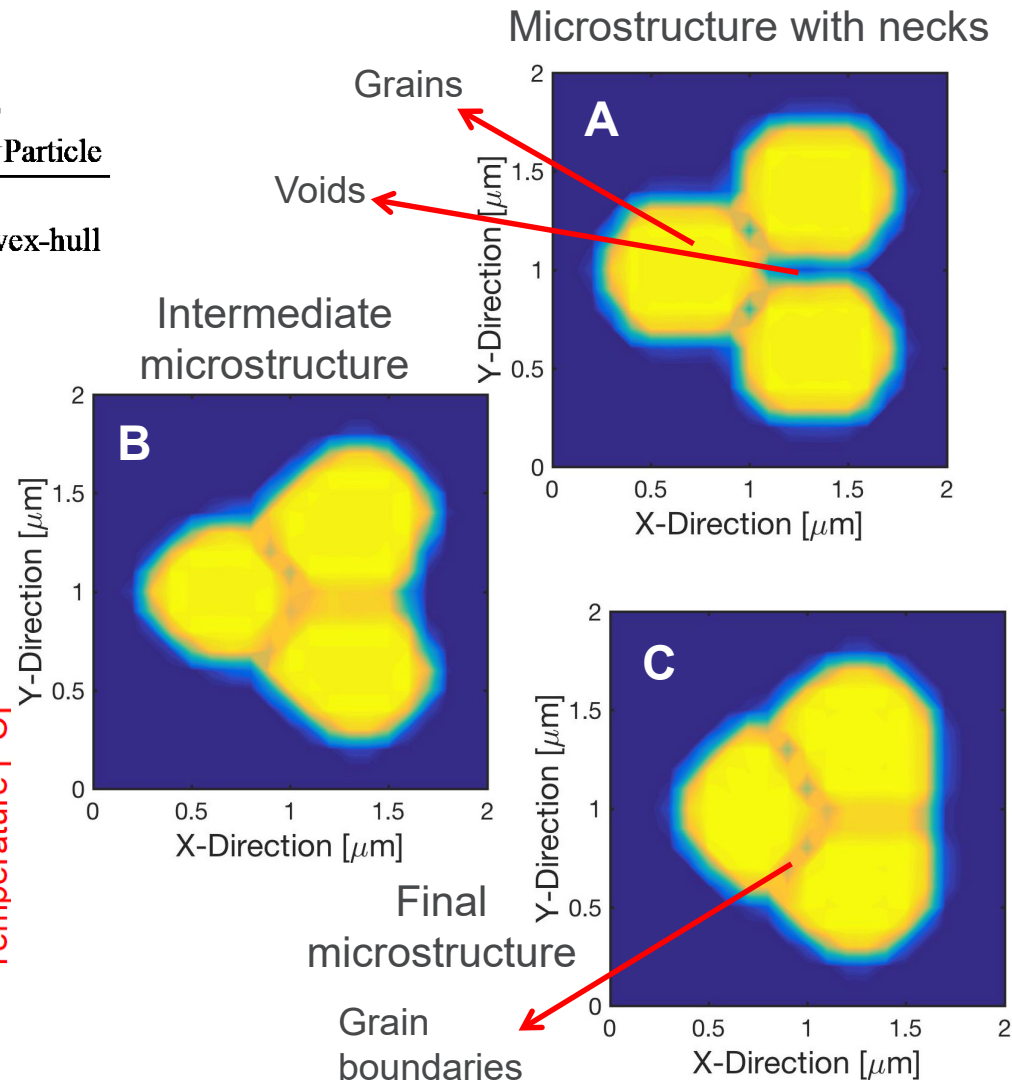
During the sintering process, smaller particles are consumed before the larger ones.

CAPTURING DENSIFICATION USING PHASE FIELD MODEL

$$\text{Relative Density} = \frac{\sum A_{\text{Particle}}}{A_{\text{Convex-hull}}}$$

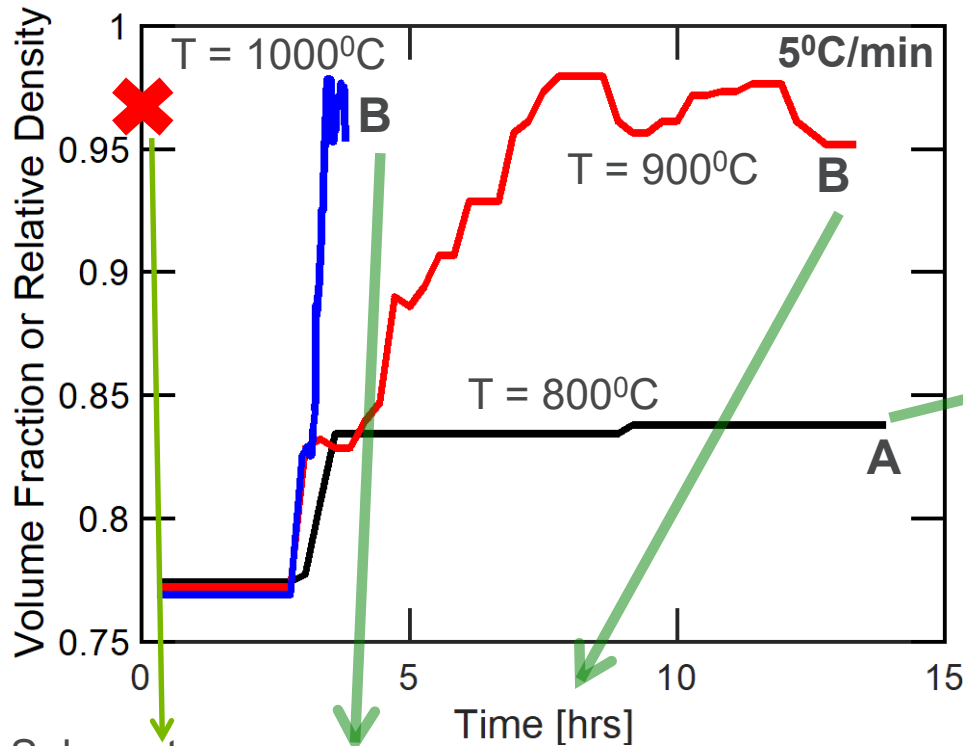


Model predicted densification during sintering of three equal sized particles

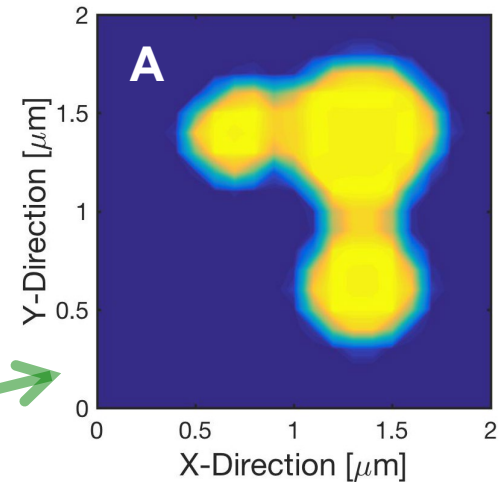
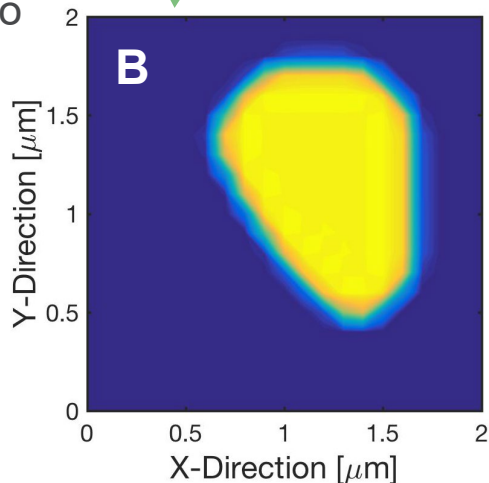


Developed model can successfully capture the various stages of densification.

COMPARISON OF DENSIFICATION AT DIFFERENT TEMPERATURES



Sakamoto
et al.



Impact of temperature taken into account as:

$$D(T) = D_0 \exp\left(-\frac{E_a}{RT}\right) \quad E_a \sim 300 \text{ kJ/mol}$$

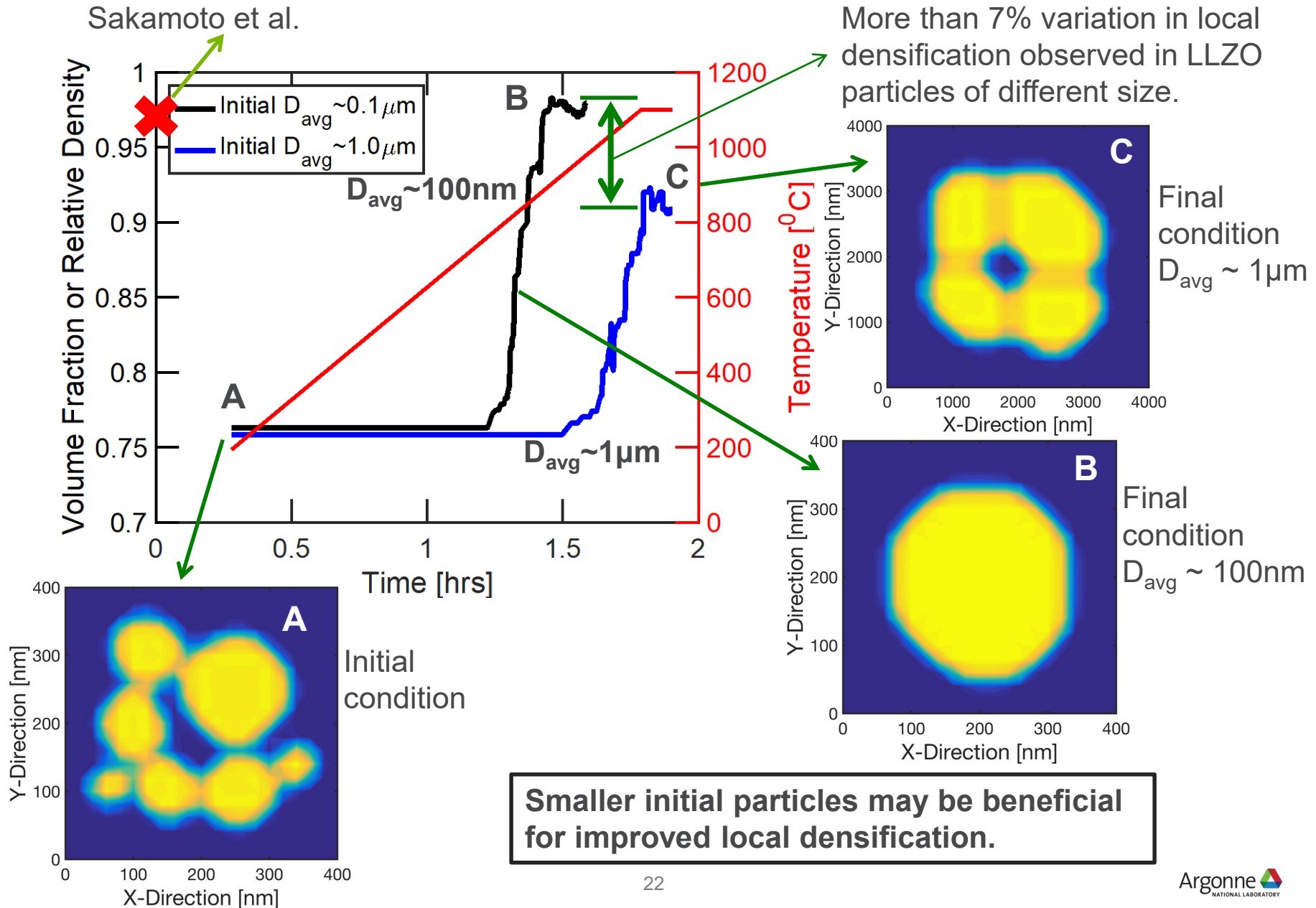
Higher the temperature, faster the densification.

- Attributed to faster transport of materials with larger diffusion coefficient.

- Present simulation, average initial particle size $\sim 400\text{nm}$
- How does initial particle size affect densification?

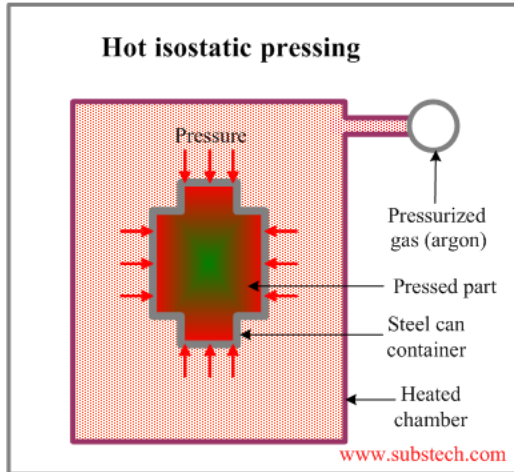
PARTICLE SIZE DEPENDENT DENSIFICATION

Sakamoto et al.



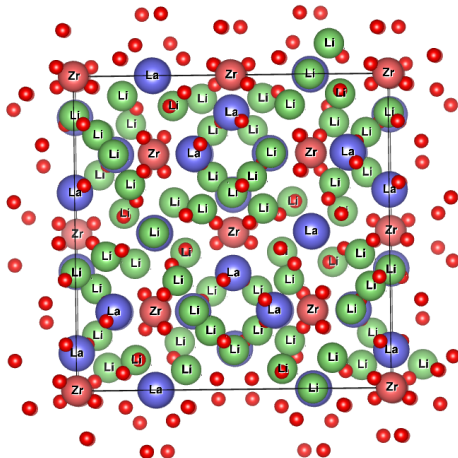
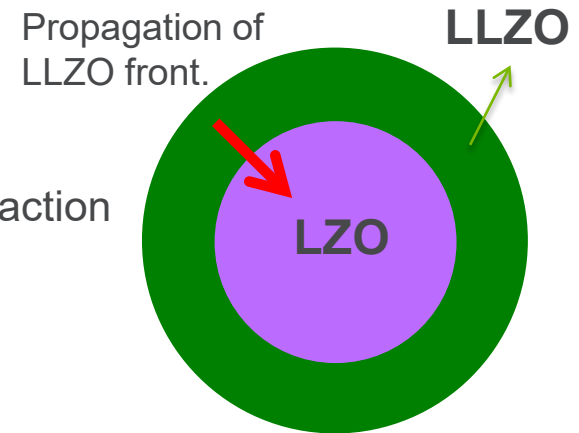
TASK: 2. FUTURE WORK POSSIBILITIES

- Experimental estimation and visualization of the densification process (at APS, ANL).



- Typically sintering is conducted using Hot Isostatic Press (HIP)
 - Add external pressure to the model

- Model formation of LLZO as a reaction propagation technique.



- Impact of Boron (B) on the synthesis and properties of LLZO (in the form of sintering aid or dopants).

RESPONSE TO PREVIOUS YEAR REVIEWER'S COMMENTS

- This is the first year of this project. Hence, no earlier comments from the reviewer.

COLLABORATION AND COORDINATION

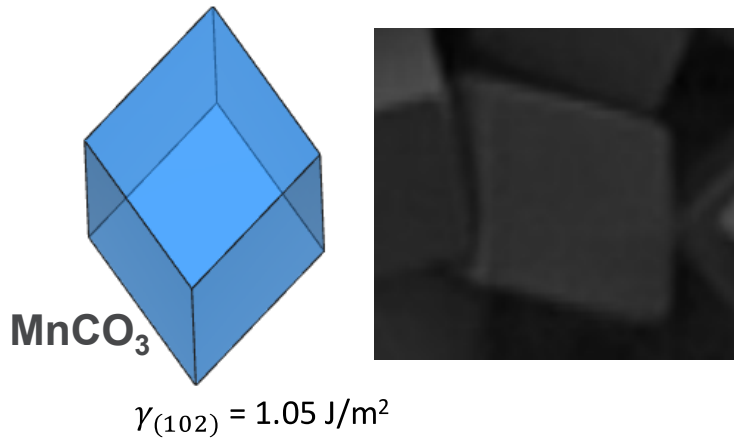
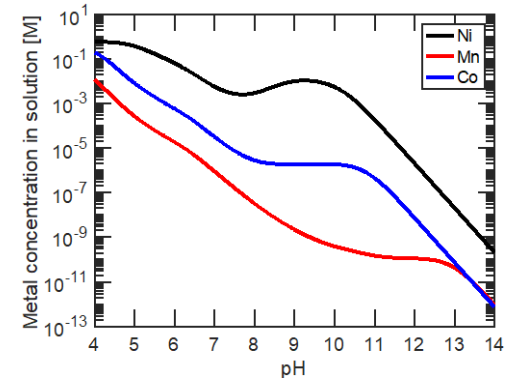
- ANL
 - Gregory Krumdick and Joseph Libera (MERF), Project ID: BAT315
 - Jason Croy and Arturo Gutierrez
- University of Chicago
 - Joanne Stubbs and Peter Eng. (APS, ANL)
- BNL
 - Feng Wang, Project ID: BAT183
- LBNL
 - Kenneth Higa
- DOE User Facility
 - Advanced Photon Source (APS), located in ANL

REMAINING CHALLENGES AND BARRIERS

- ❑ The developed DFT based atomistic modeling technique assumes only the reaction with hydrogen and/or oxygen while estimating the equilibrium configuration of precursors. However, in the presence of carbonate ions in the solution, the entire carbonate molecule can detach or reattach with the particle surface, which can significantly impact its surface energy and equilibrium shape.
- ❑ The phase field based methodology assumes the presence of a very few number of particles (around 5 to 10) within the computational domain. However, during experiment millions of particles participate in the sintering process.
 - In order to capture the collective behavior of all the grains, a homogenized sintering model should be developed.
- ❑ Estimation of exact grain-boundary mobility during sintering, or measurement of particle shape evolution during coprecipitation and/or sintering, has not been attempted, but should be addressed for obtaining a good set of experimental data that can inform the computational models regarding the relevant physics.

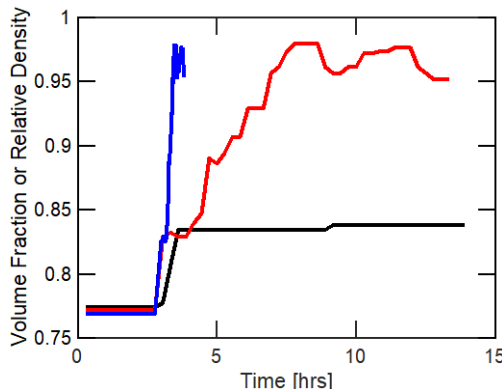
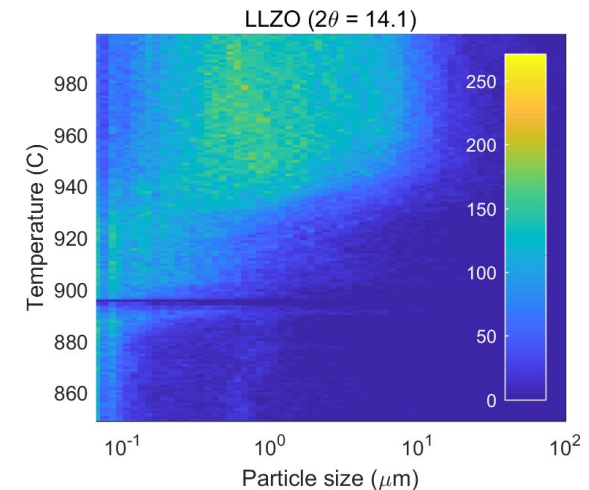
SUMMARY

By solving equilibrium relations, it is possible to estimate the amount of metal that precipitate under certain solution pH.



Equilibrium Wulff shapes have been estimated for the cathode precursor primary particles, which correlate very well with experimental observations.

In situ experiments conducted at APS reveal the grain ripening behavior of LLZO during high temperature sintering.



Developed phase field based computational models can capture the densification phenomena successfully.